

Полупроводниковые метаповерхности для нелинейной фотоники

Андрей Федянин

Физический факультет МГУ

nanolab.phys.msu.ru



Полупроводниковые метаповерхности для нелинейной фотоники и оптических аналоговых вычислений

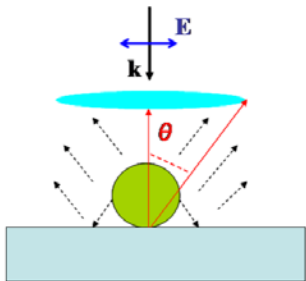
Андрей Федянин

Физический факультет МГУ

nanolab.phys.msu.ru

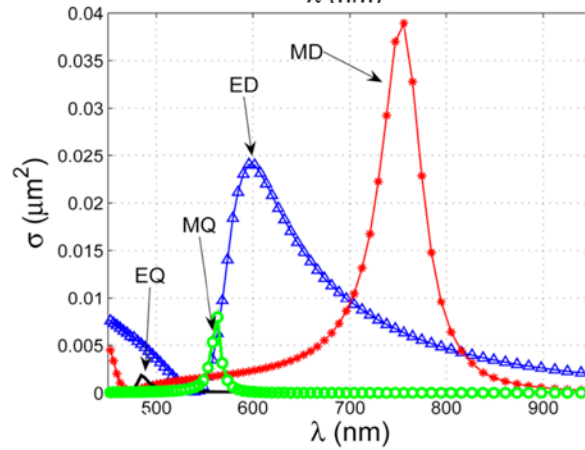
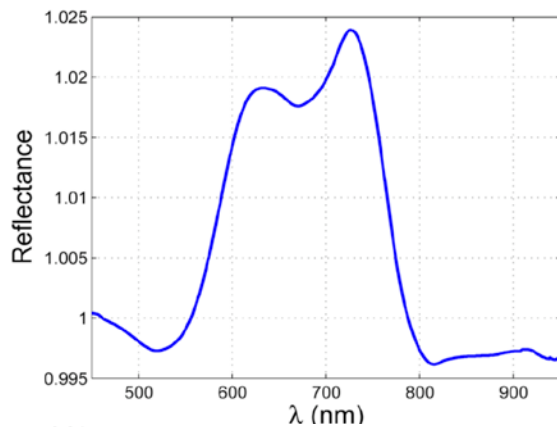


Mie scattering. Basics

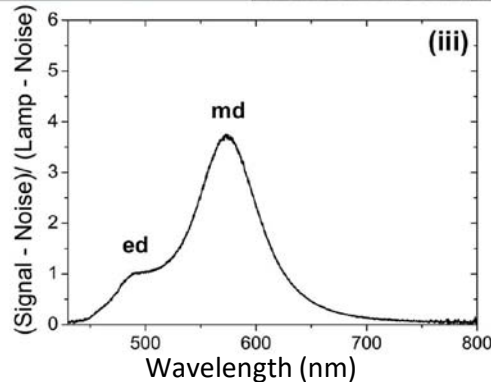
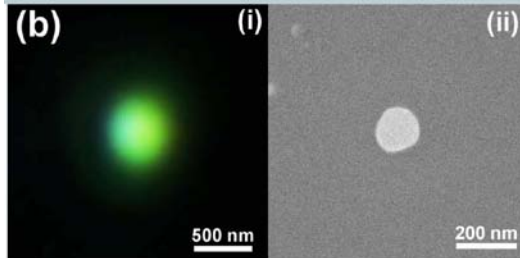
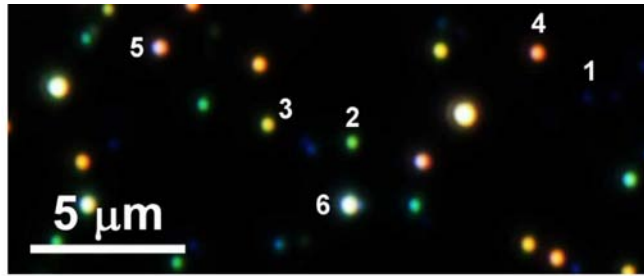


$$\mathbf{E}(\mathbf{r}) = \frac{k_0^2 e^{ik_0 r}}{4\pi\epsilon_0 r} ([\mathbf{n} \times [\mathbf{p} \times \mathbf{n}]] +$$
$$+ \frac{ik_0}{6} [\mathbf{n} \times [\mathbf{n} \times \hat{Q}\mathbf{n}]] +$$
$$+ \frac{1}{c} [\mathbf{m} \times \mathbf{n}] + \frac{ik_0}{2c} [\mathbf{n} \times (\hat{M}\mathbf{n})])$$

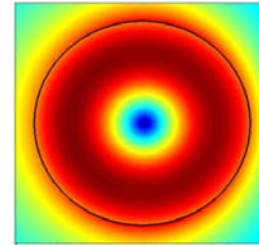
A.B. Evlyukhin et al.,
Nano Letters **12**, 3749 (2012)



Mie-type resonances in high-index nanoparticles

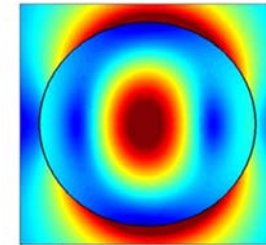


(1) Magnetic dipolar

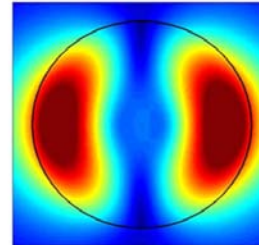


$|E|^2$ maps

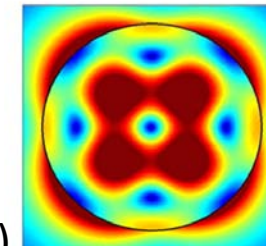
(2) Electric dipolar



(3) Magnetic quadrupolar

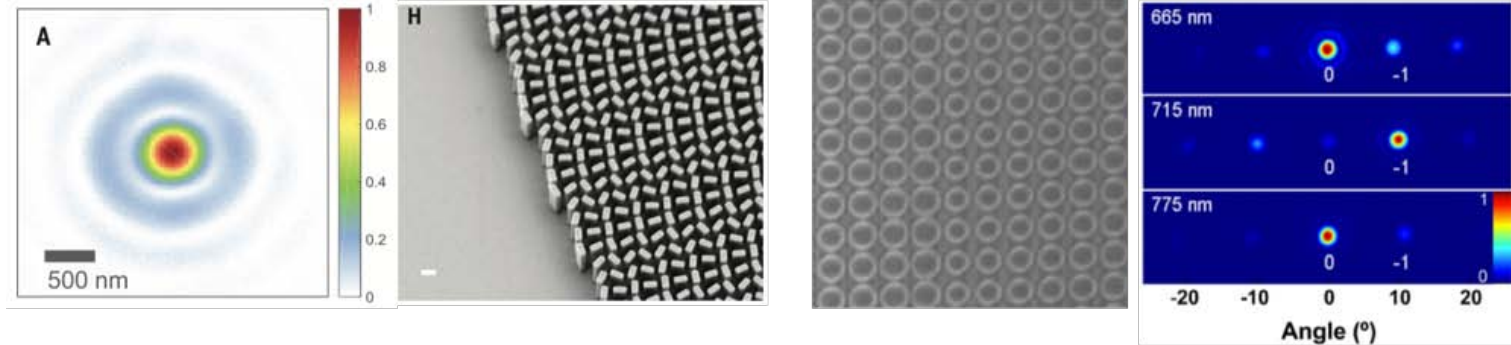


(4) Electric quadrupolar



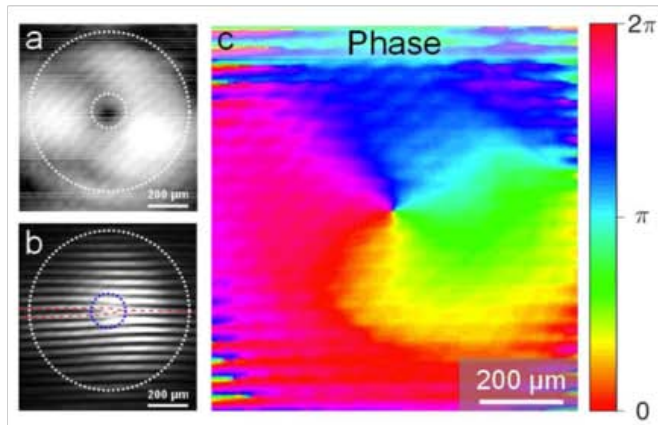
Kuznetsov et al.,
Sci. Rep. **2**, 492 (2012)

All-dielectric photonic metasurfaces

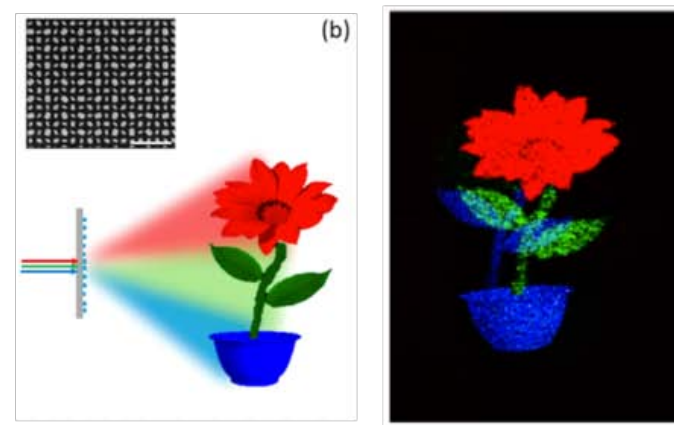


M. Khorasaninejad et al., Science 352, 1190 (2016)

Y.F. Yu et al., Las. Phot. Rev. 9, 412 (2015)



K. Chong et al., Nano Lett. 15, 5369 (2015)



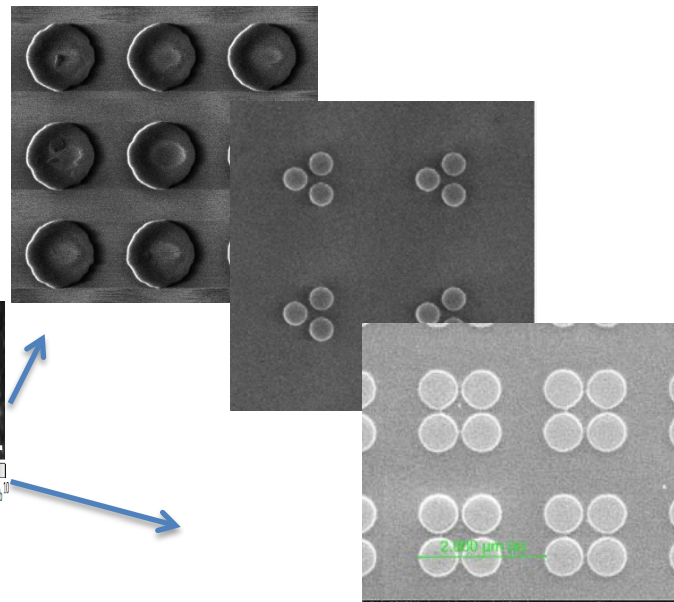
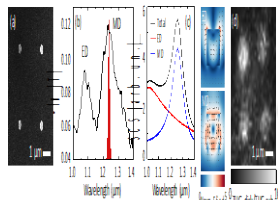
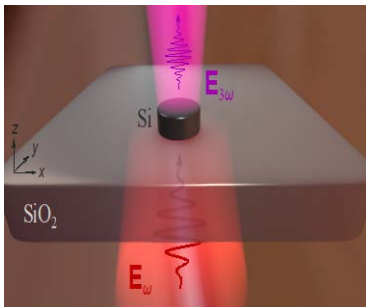
B.Wang et al., Nano Lett. 16, 5235 (2016)

Nonlinear optics of Mie-resonant nanoparticles

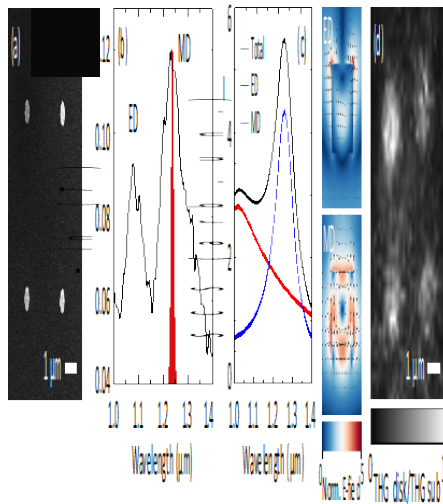
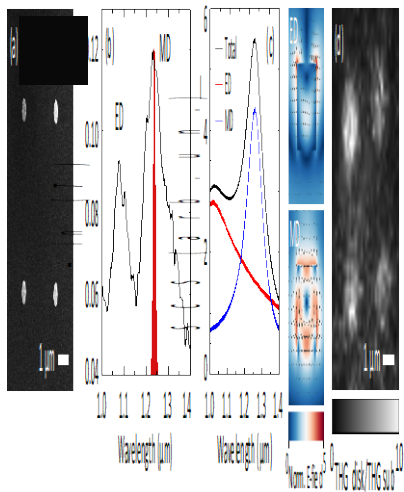
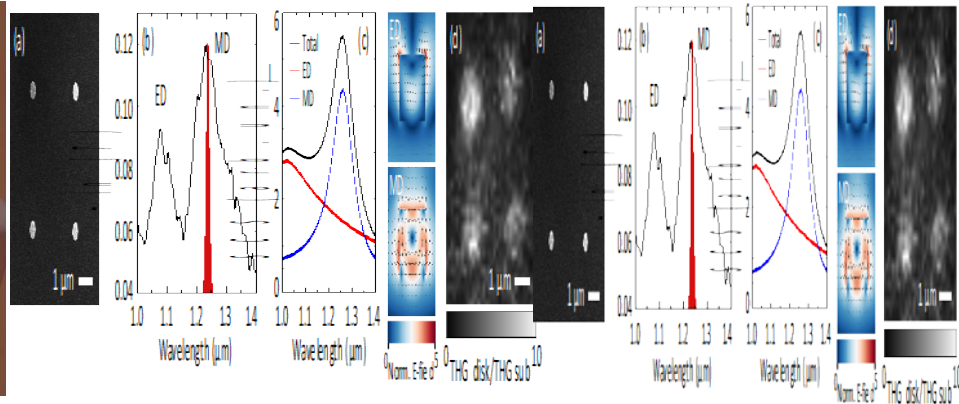
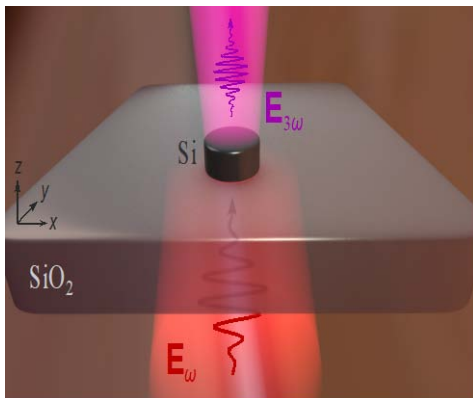
Goals:

- Nonlinear optical enhancement
- Magnetic vs. electric resonances
- Coupled nanoparticles: oligomers and metasurfaces

- small values of $\chi^{(2)}$ and $\chi^{(3)}$
- small volumes
- no phase matching

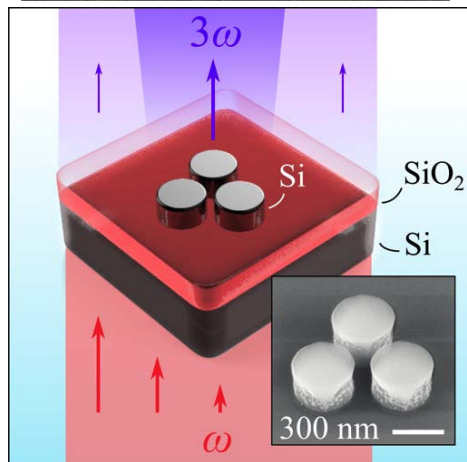
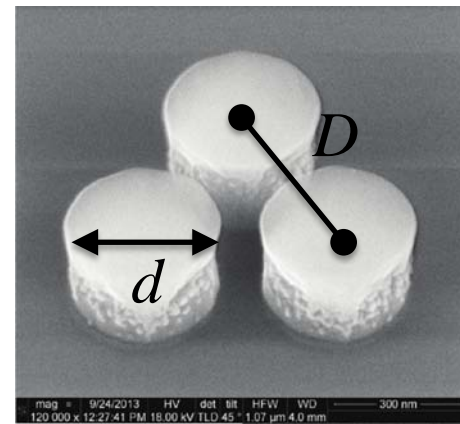
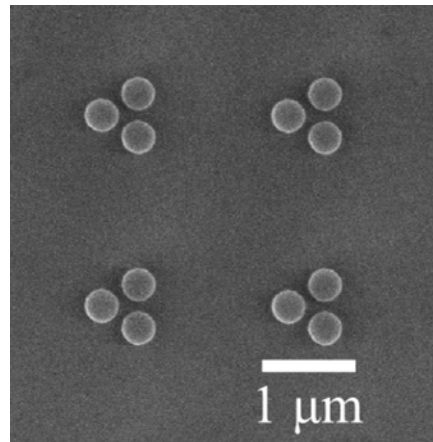
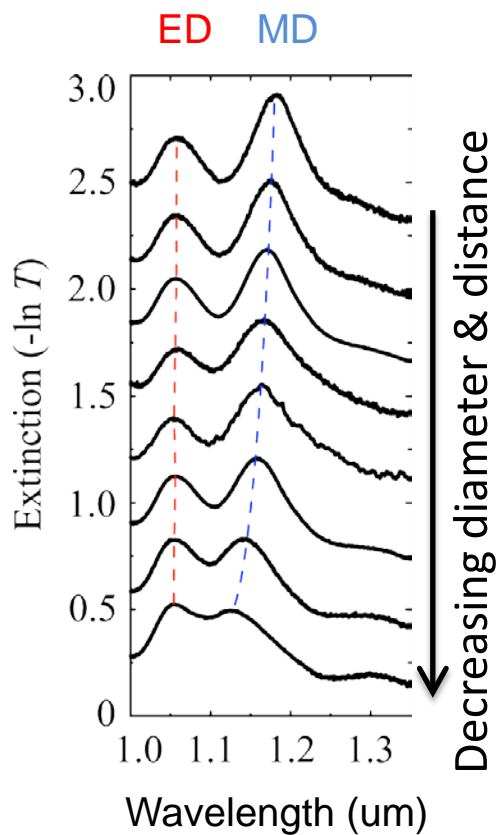


Third-harmonic generation confocal microscopy



Olympus FluoView
FV1000
+ Coherent
Chameleon Ultra II
+ Coherent OPO
pump @ 1240 nm

Silicon nanodisk trimers sample design

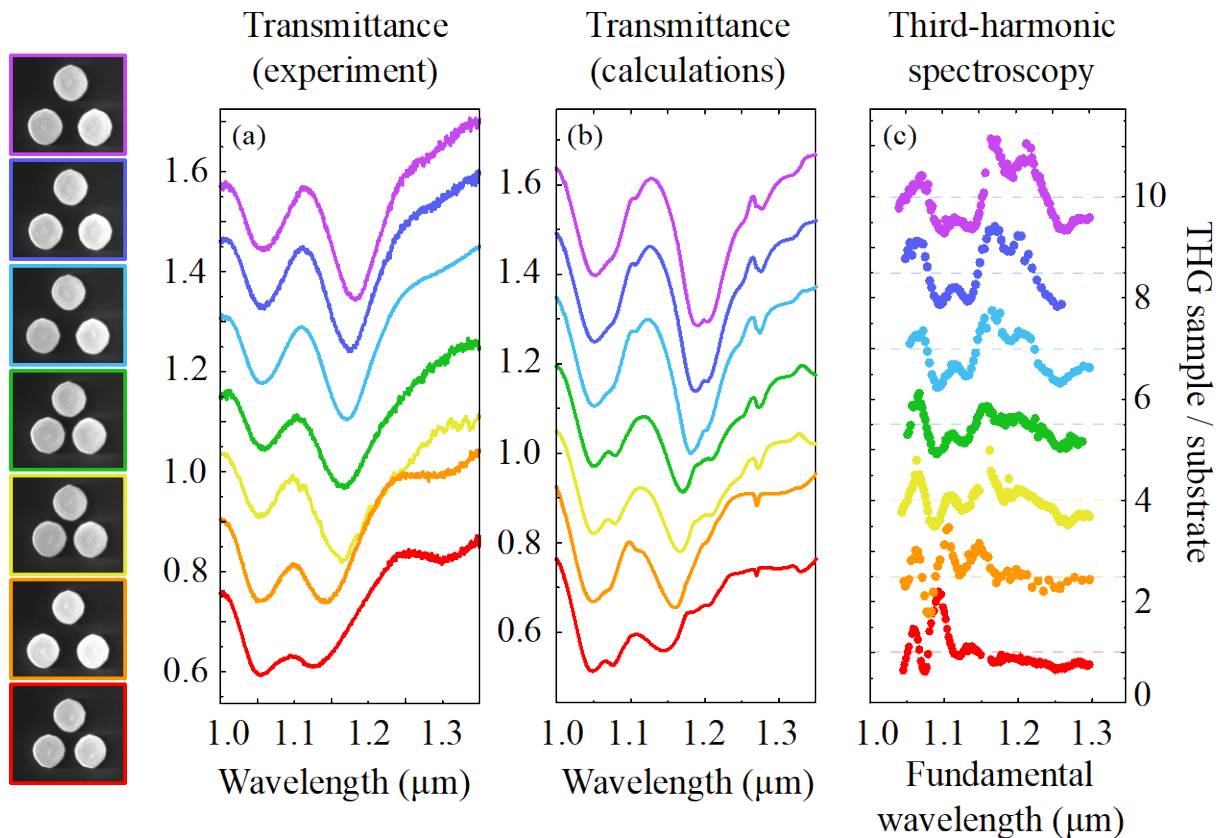


Different d and D sets:

$d = 350\text{--}375\text{ nm}$

$D = 460\text{--}560\text{ nm}$

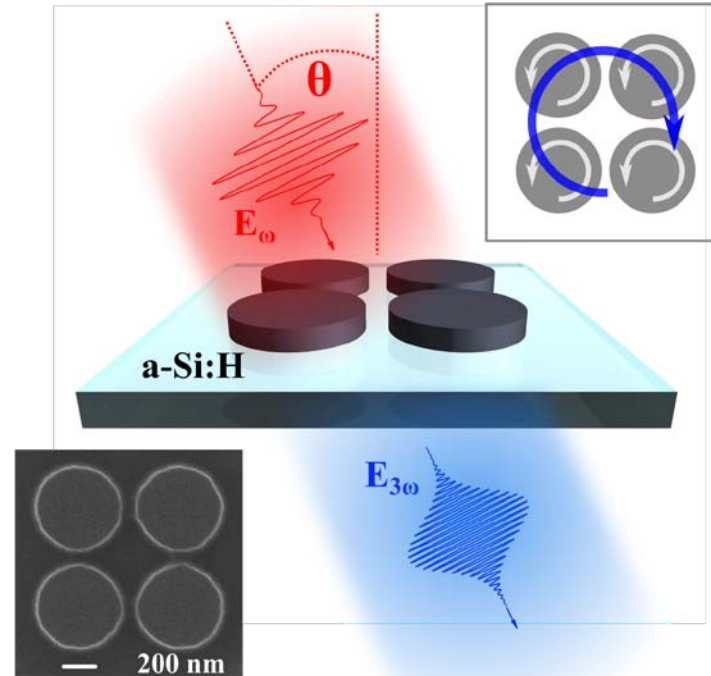
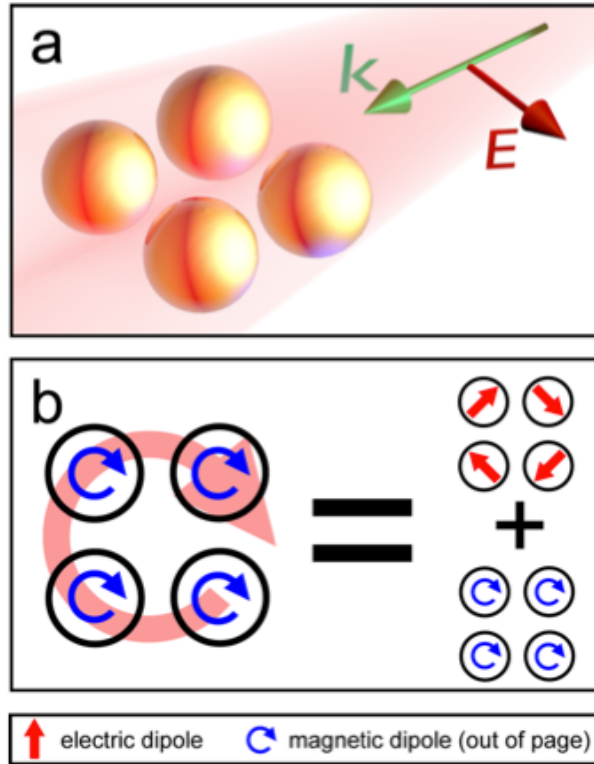
THG spectroscopy of silicon trimers



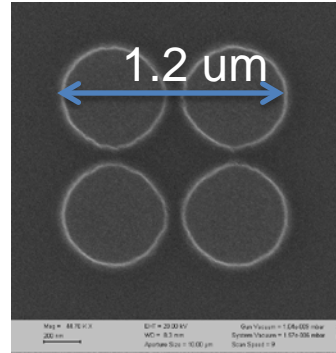
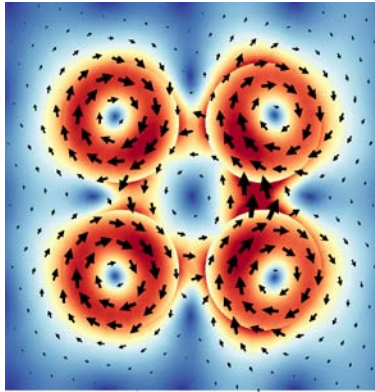
ACS Photonics **2**, 578 (2015)

Phil. Trans. R. Soc. A **375**, 20160281 (2017)

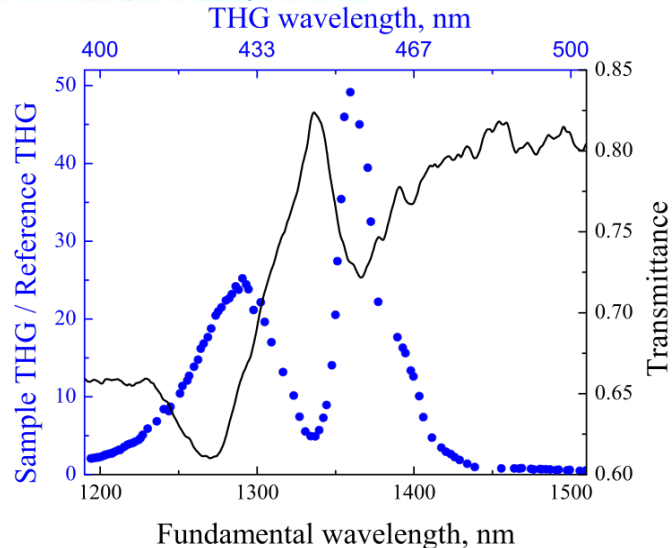
Quadrumers: optical retardation and collective resonance



THG enhancement at magnetic Fano resonance



- Amorphous silicon
- Resonance spectrum = spectrum of the pulse
- Low TH absorption



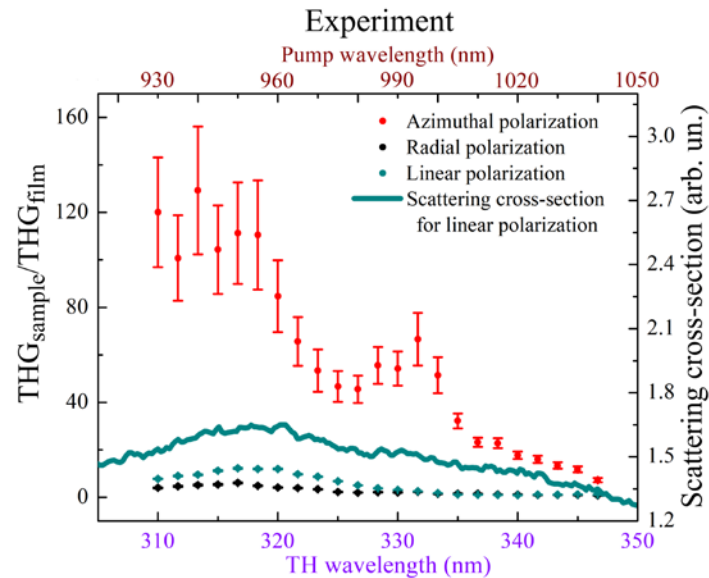
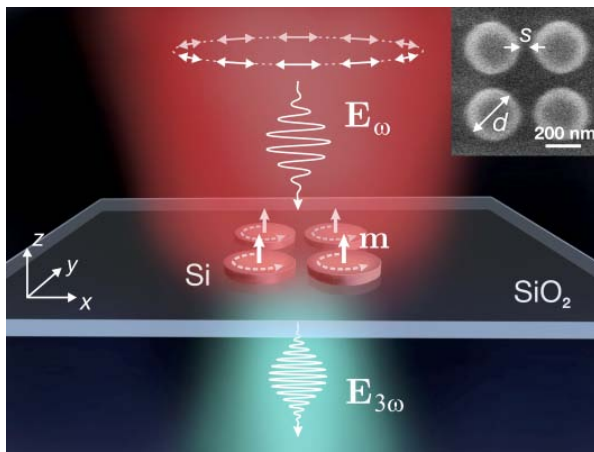
IR to blue conversion $\sim 10^{-5}$

Record set for
a silicon subwavelength object

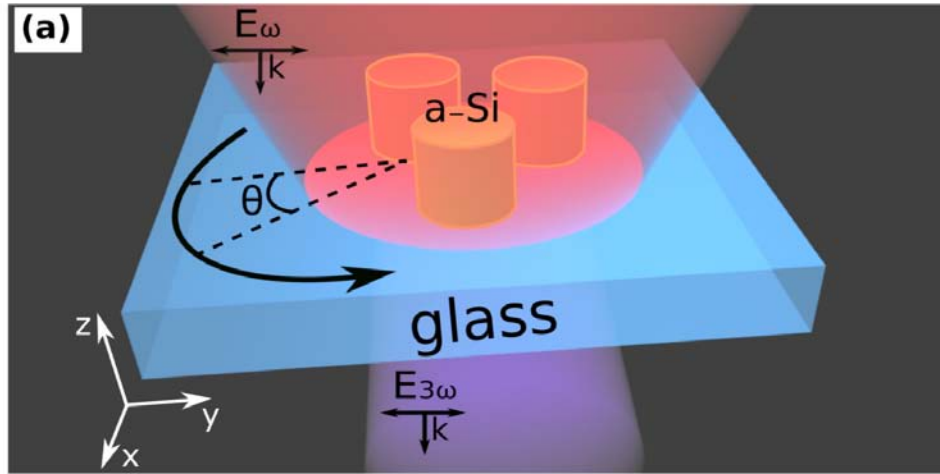
Nano Letters **16**, 4857 (2016)

Nano Letters **20**, 3471 (2020)

Enhanced Nonlinear Light Generation in Oligomers under Vector Beam Illumination

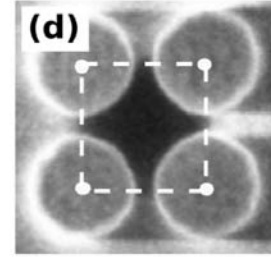
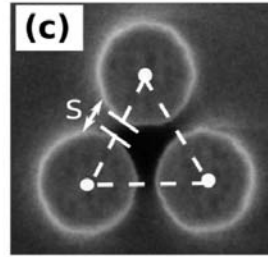
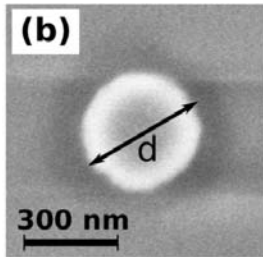


Tailored nonlinear anisotropy in Mie-resonant dielectric oligomers

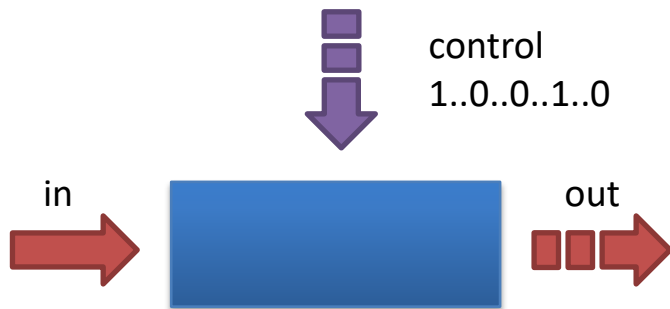


Idea:

- linear scattering remains isotropic
- azimuthal dependence of THG signal reflects their point-group symmetry



All-optical switching by nanophotonic elements



coherent approaches

- via wave mixing or other multiphoton processes
- no relaxation time

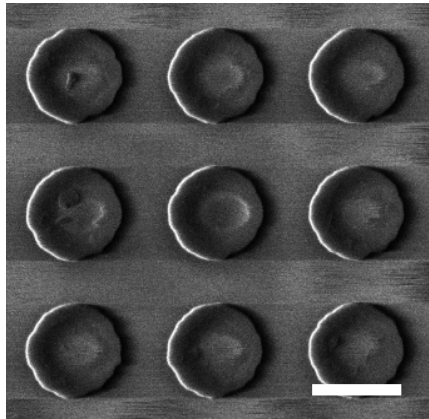
incoherent approaches

- via solid-state excitations
- relaxation time is a strong limiting factor

All-optical switching in Si and GaAs metasurfaces

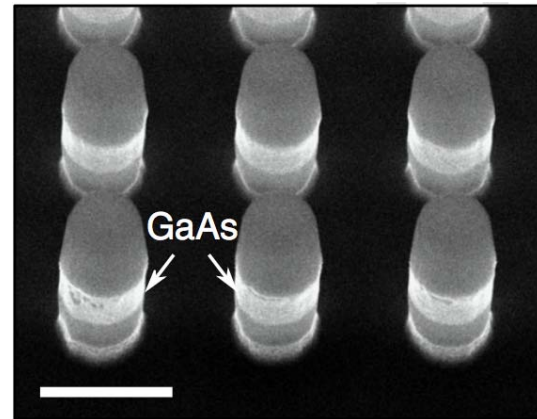
- Two-photon absorption enhancement observation in Mie-resonant Si metasurfaces
- Free-carrier-induced ultrafast tuning of direct band gap GaAs metasurface

silicon



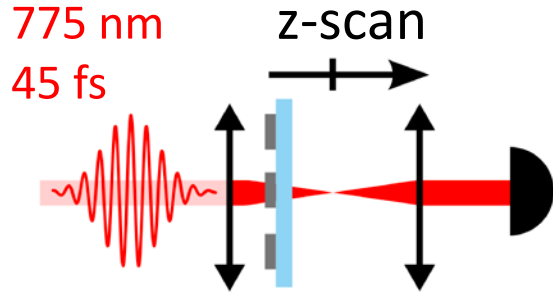
Nano Letters **15**, 6985 (2015)

gallium arsenide

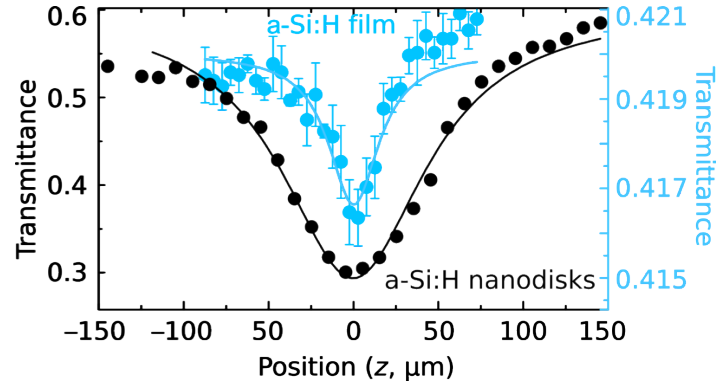
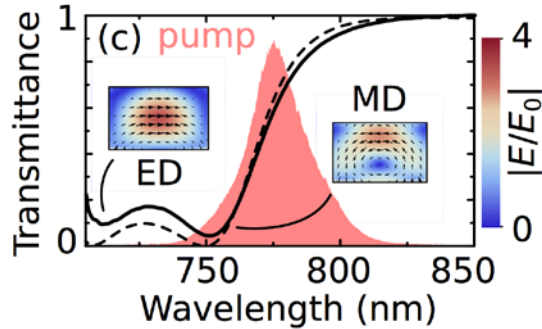


Nature Commun. **8**, 17 (2017)

Nonlinear absorption: $\text{Im } \chi^{(3)}(\omega = \omega + \omega - \omega)$. Silicon

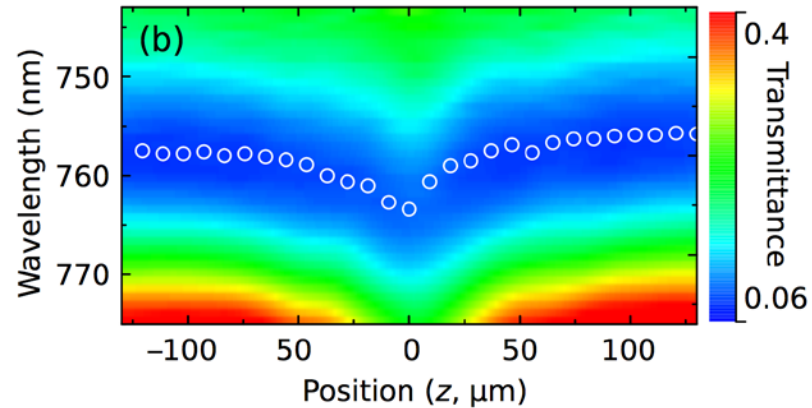


$$T(z) = 1 - \frac{1}{2\sqrt{2}} \frac{\beta_{\text{sam}} IL}{1 + \left(\frac{z}{z_0}\right)^2}$$

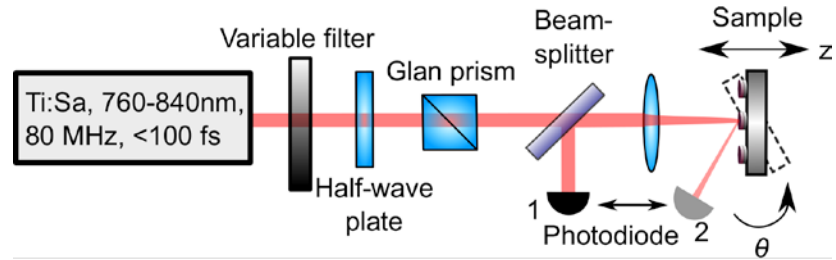


$$\beta_{\text{film}} = 0.07 \text{ cm/kW}$$

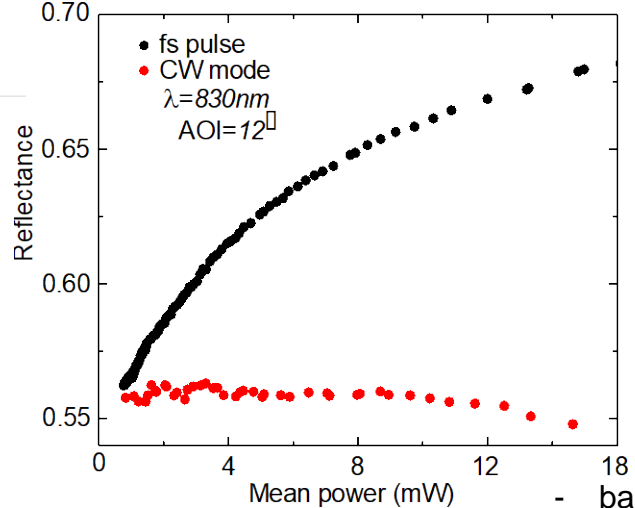
$$\beta_{\text{sam}} = 5.6 \text{ cm/kW (film x80)}$$



Intensity dependent reflectance. Gallium Arsenide



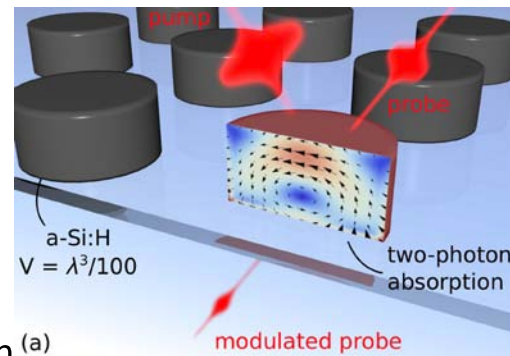
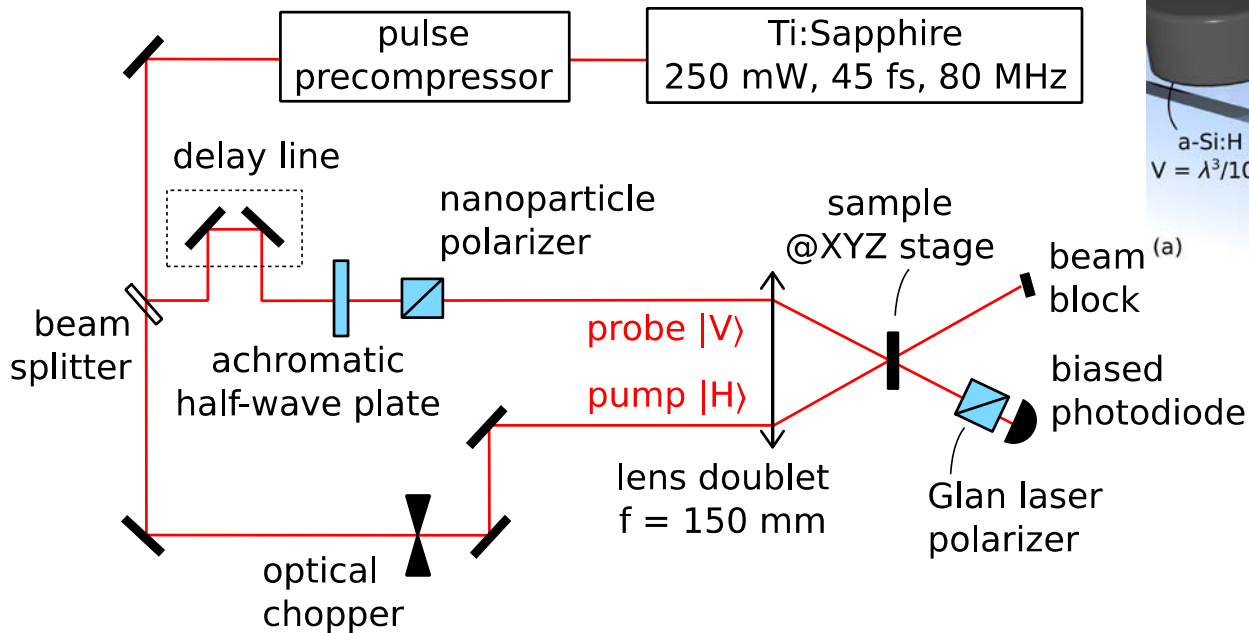
FS pulse mode vs CW mode



- band filling
- bandgap shrinkage
- Drude term

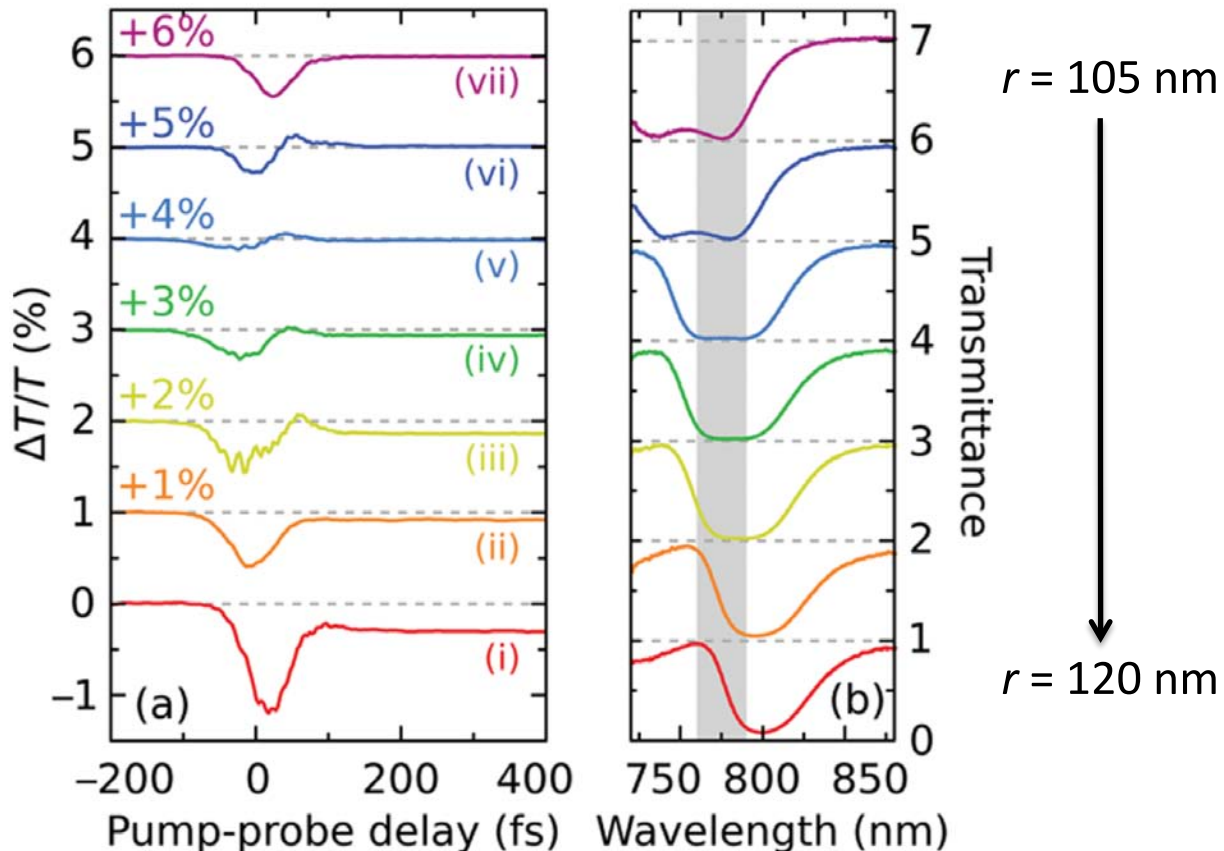
$$\uparrow I \square \uparrow N_{free-carr} \square \Delta\kappa, \Delta n$$

Frequency-degenerate pump-probe spectroscopy

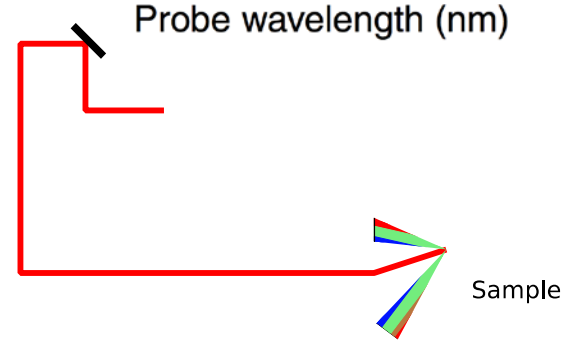
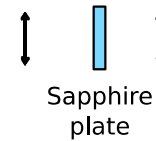
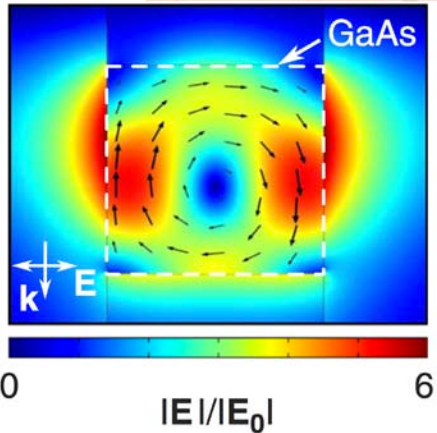
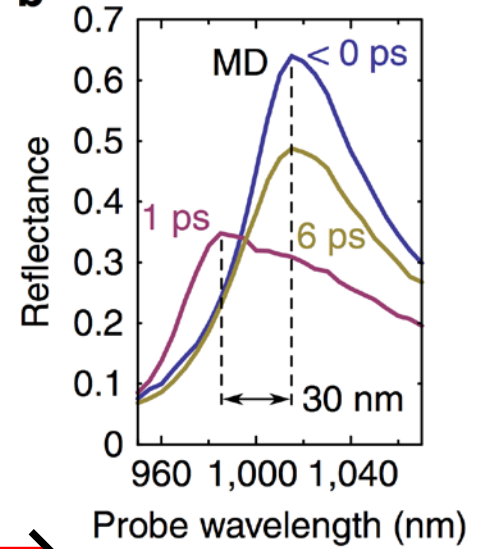
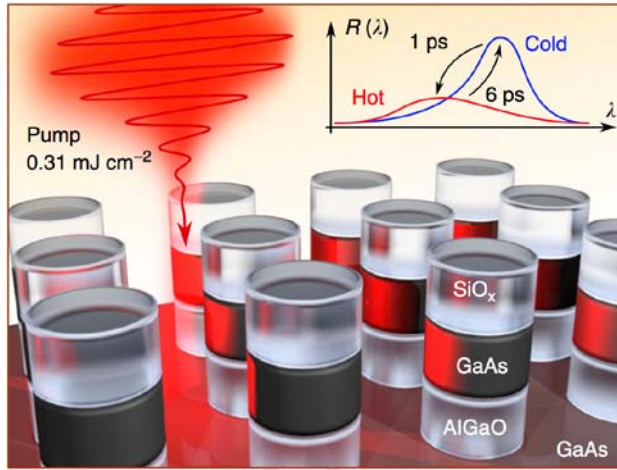


13 fJ per disk

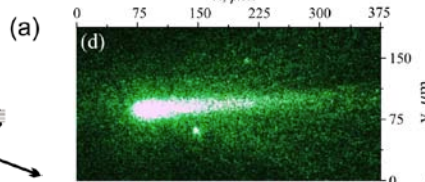
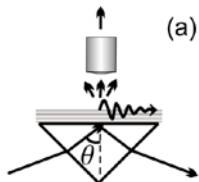
Frequency-degenerate pump-probe



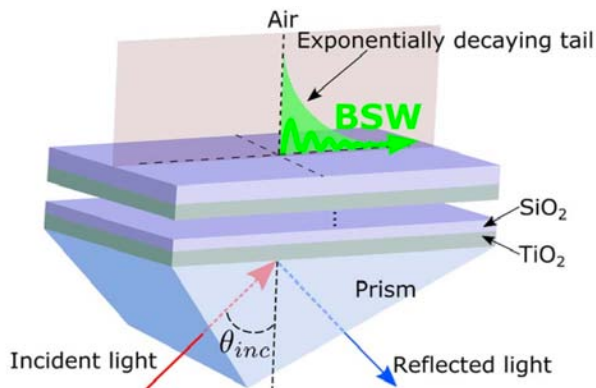
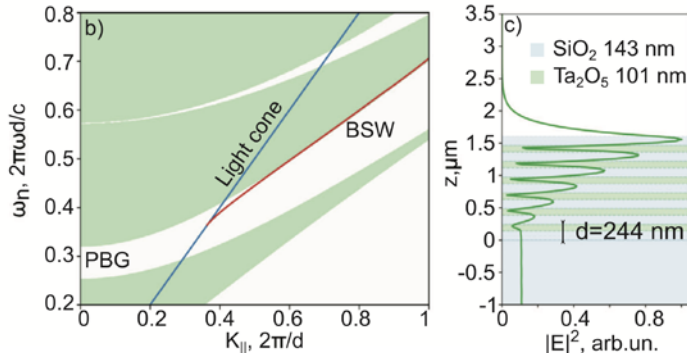
Pump-probe spectroscopy with supercontinuum probe



Bloch surface waves



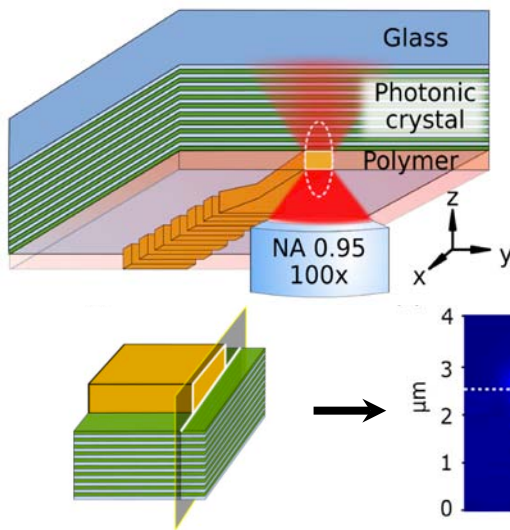
I. Soboleva et al. PRL **108**, 123901 (2012)



BSW advantages

- light localization on the surface
- no absorption
- long propagation distance (> cm in experiments)
- arbitrary spectral range (from UV to mid IR and THz)
- TE- and TM-polarized BSW
- narrow spectral and angular resonance
- wide variety of PC materials

V. Koju, W. Robertson Opt. Lett. (2016)



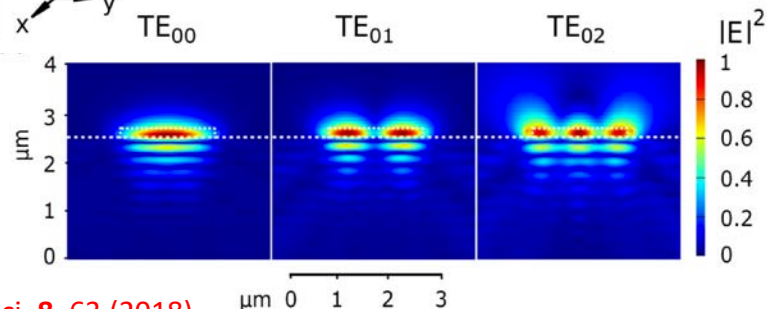
K. Abrashitova et al. Appl. Sci. **8**, 63 (2018)

Applications of BSW:

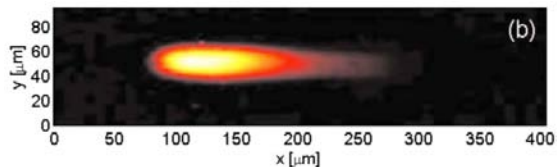
- sensing
- enhancing light-matter interaction
- SERS
- optical manipulation
- **integrated photonics**

BSW waveguides on top of PC can be made of low-refractive-index materials

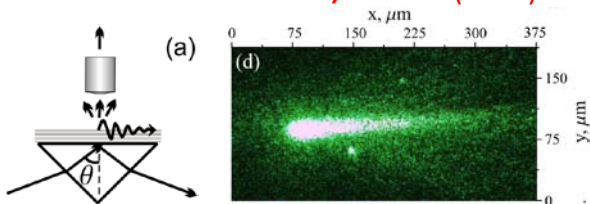
Two-photon lithography for printing single-mode and multimode BSW waveguides



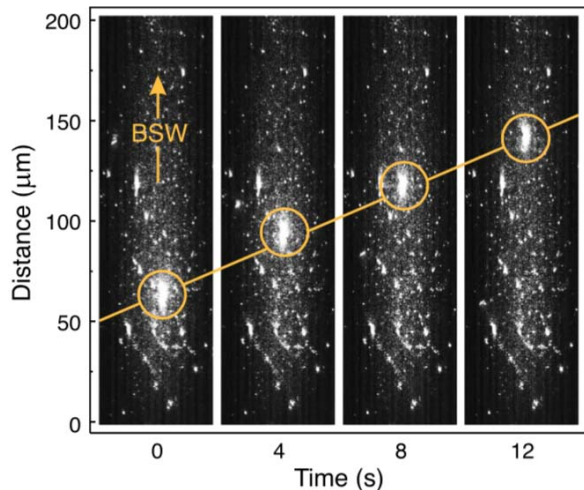
Bloch surface waves



I. Soboleva et al. *APL* **94**, 231122 (2009)



I. Soboleva et al. *PRL* **108**, 123901 (2012)

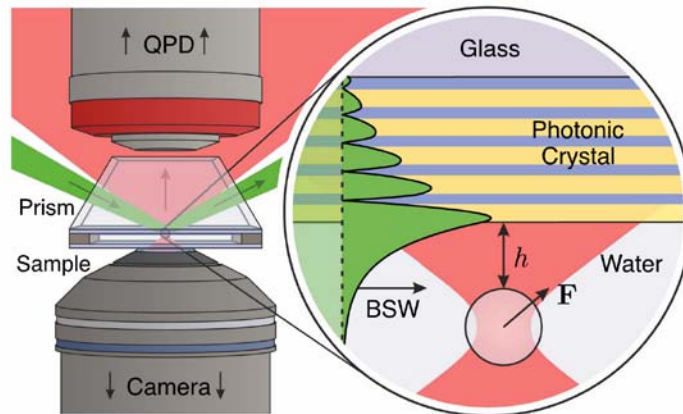


D. Shilkin et al. *Opt. Lett.* **40**, 4883 (2015)

- BSW visualization via enhanced fluorescence

- Giant Goos-Hanchen Effect

- Direct measurements of forces induced by BSW



Optical Forces

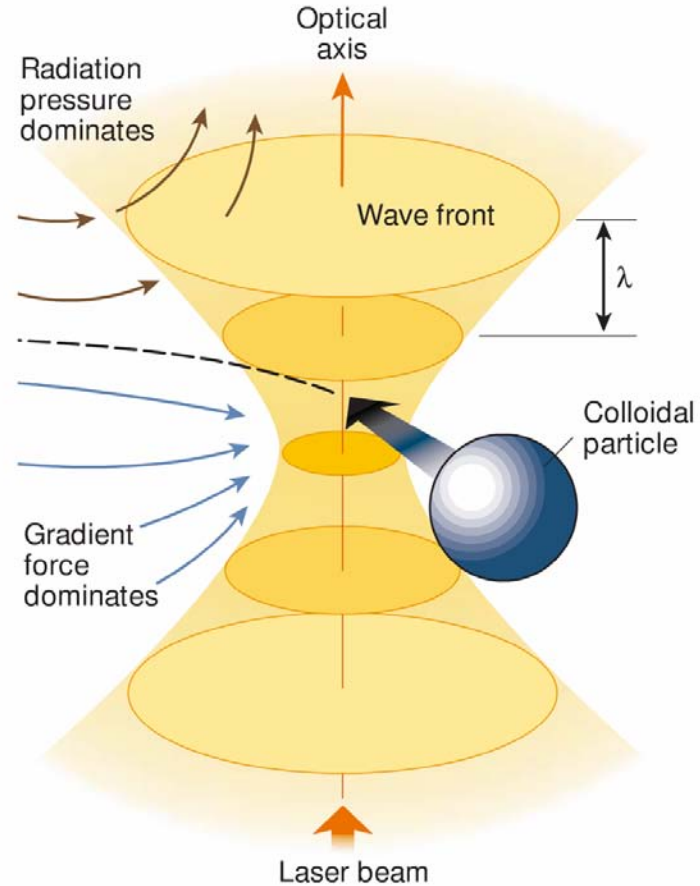
used for optical manipulation
are divided into the gradient
and the scattering components

$$F_{grad} \propto \nabla E^2$$

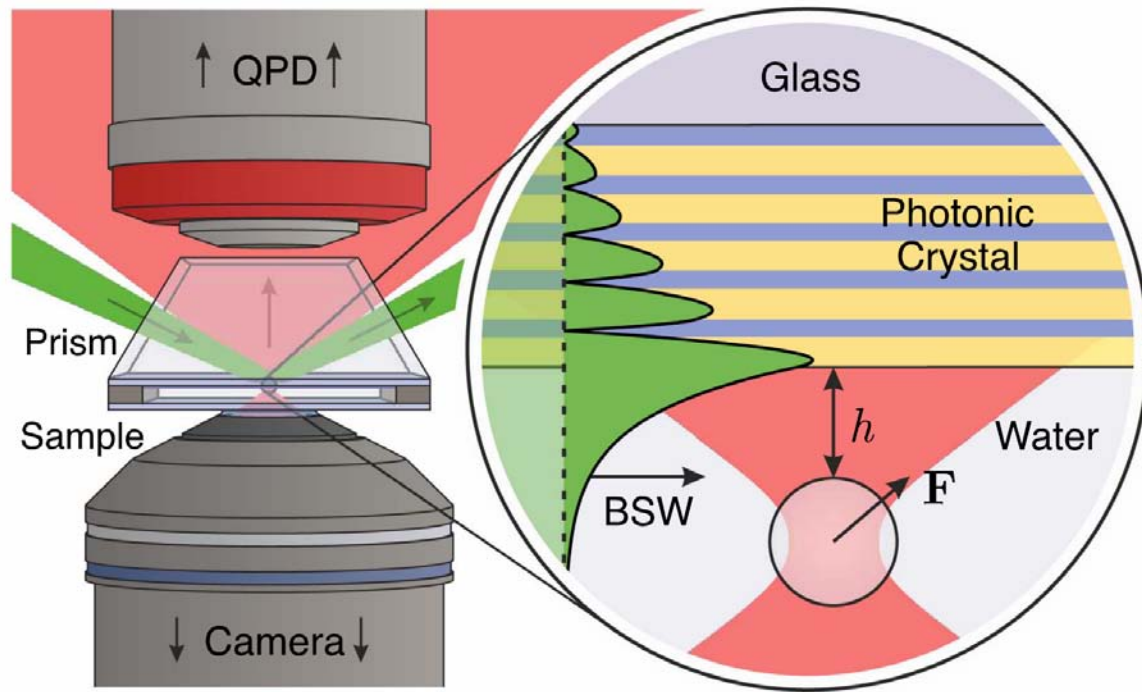
$$F_{scat} \propto E^2$$

Optical tweezers:
trapping particles
with a tightly focused
laser beam

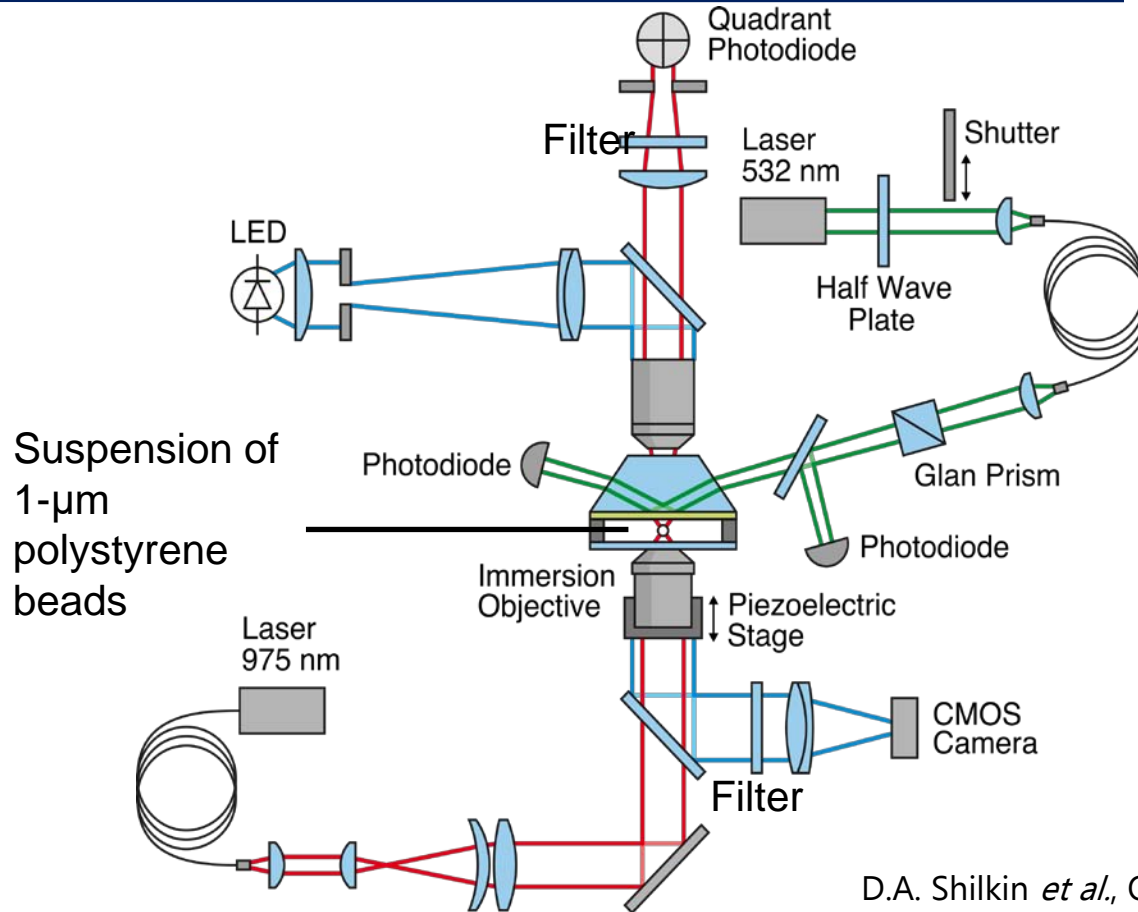
D.G. Grier, Nature **424**, 810 (2003)



Experimental Setup: the Idea

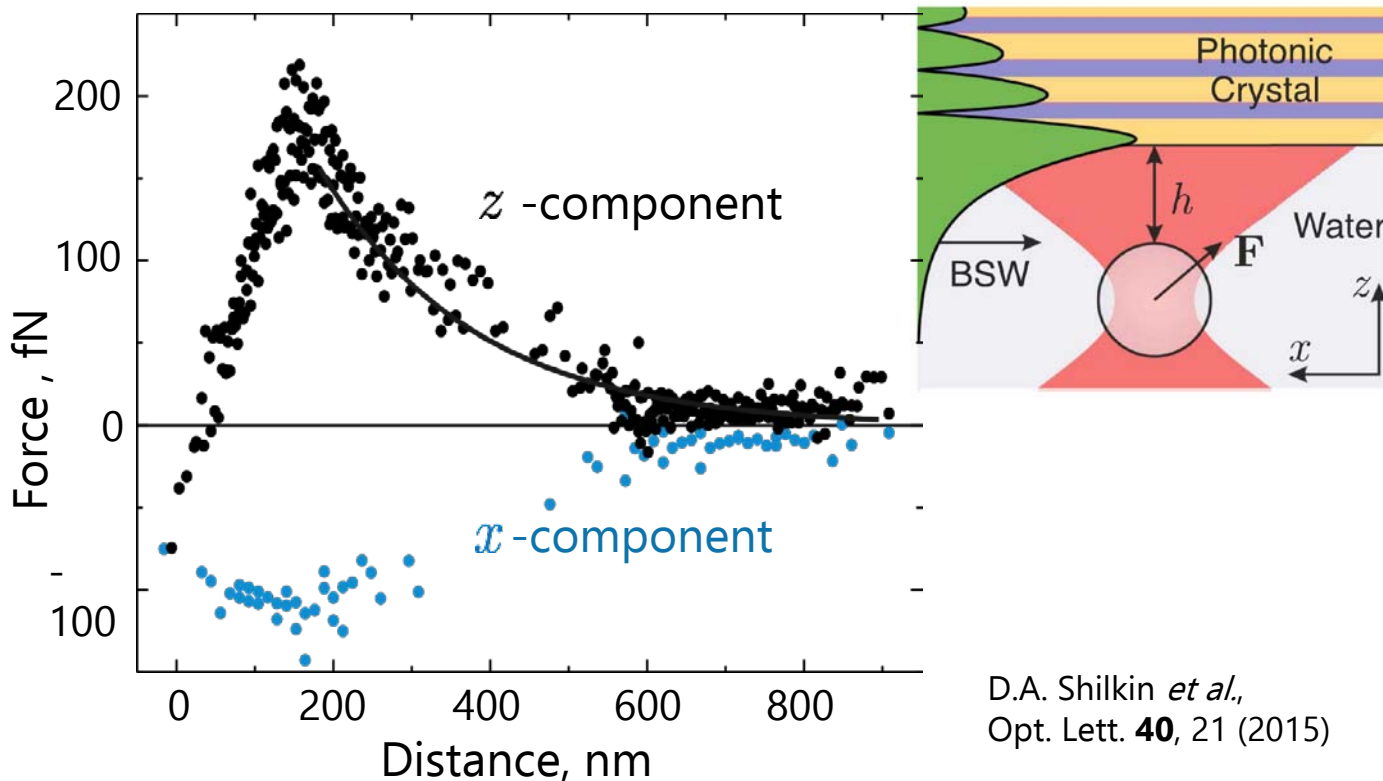


Experimental Setup: Realization



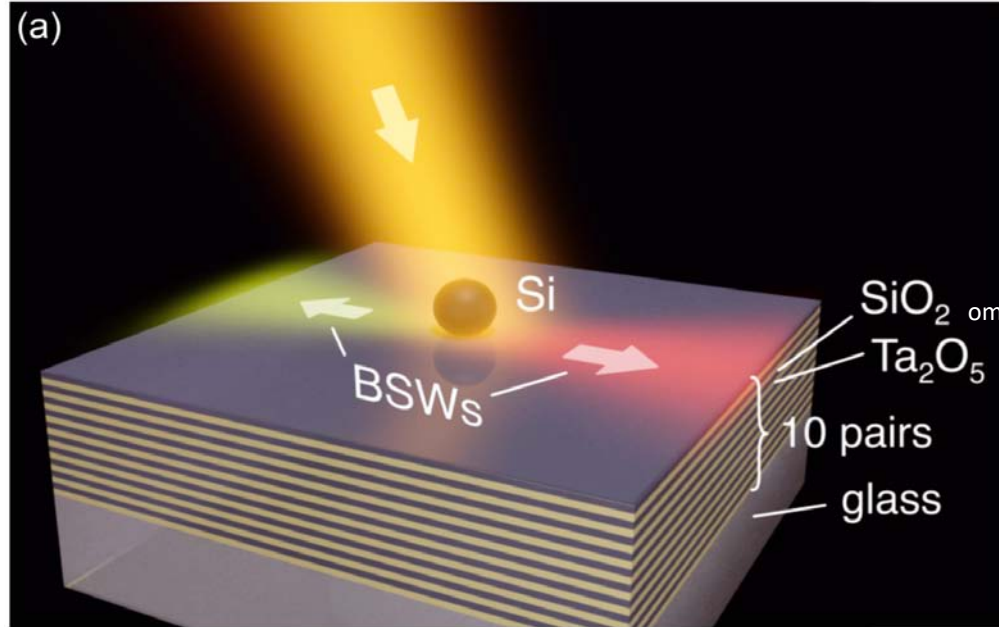
Photonic Force Microscopy with BSW

exponential decay at large distances and a surprising decrease at small ones

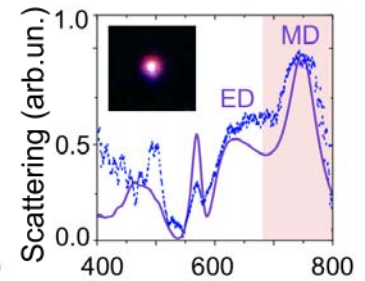
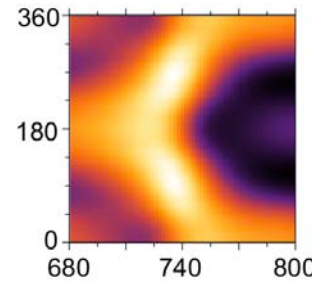
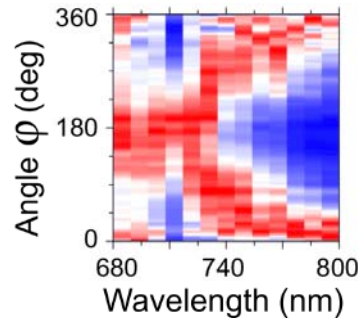
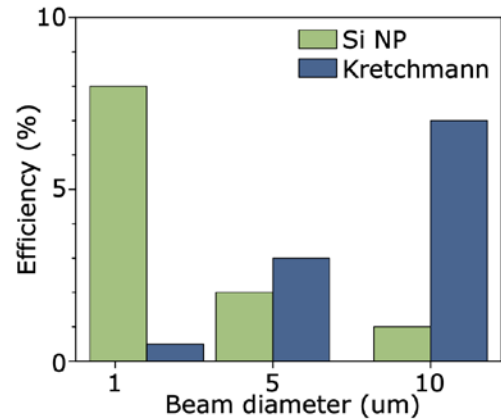
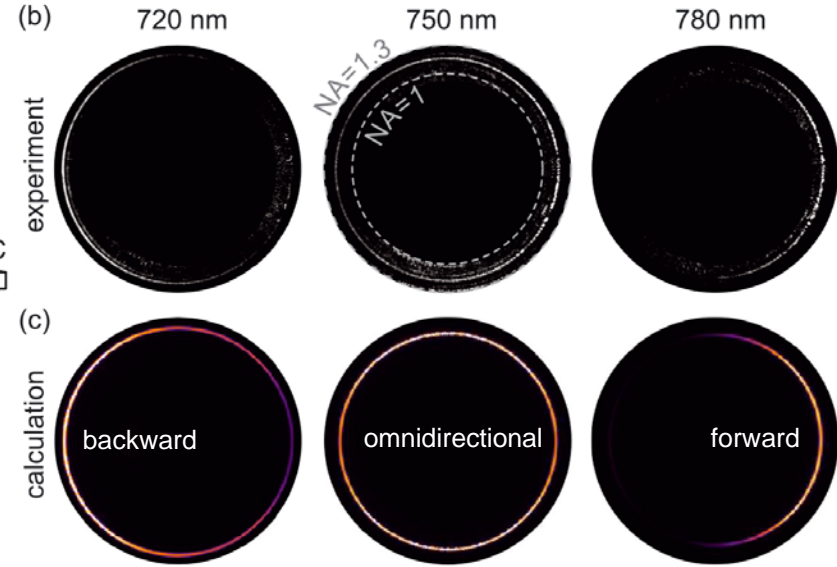
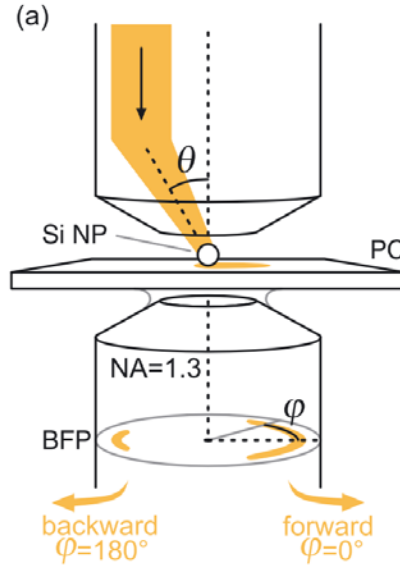
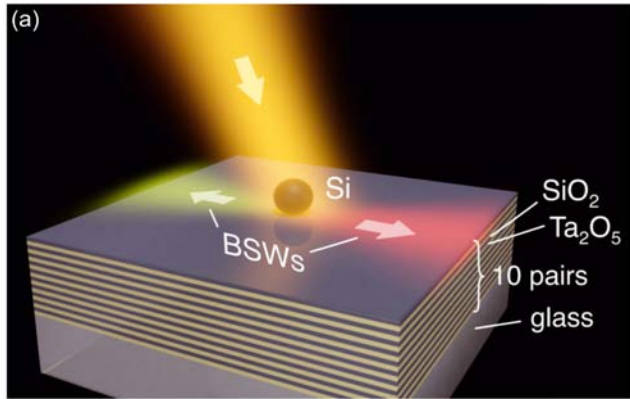


D.A. Shilkin *et al.*,
Opt. Lett. **40**, 21 (2015)

Mie-driven directional nanocoupler for BSW photonic platform

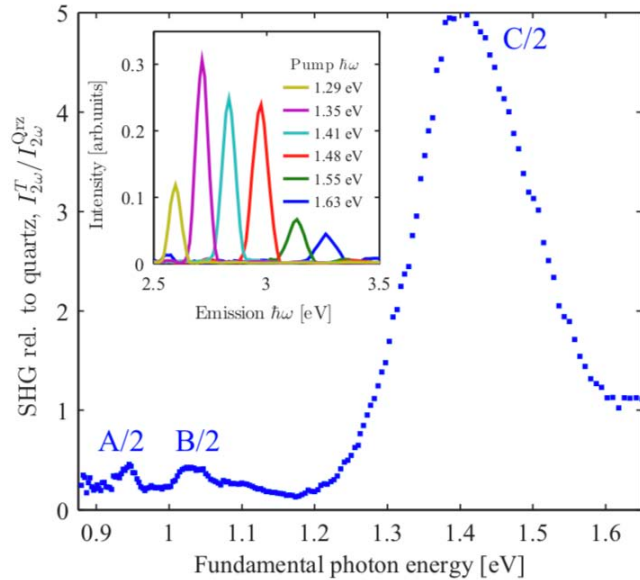


Mie-driven directional nanocoupler for BSW photonic platform



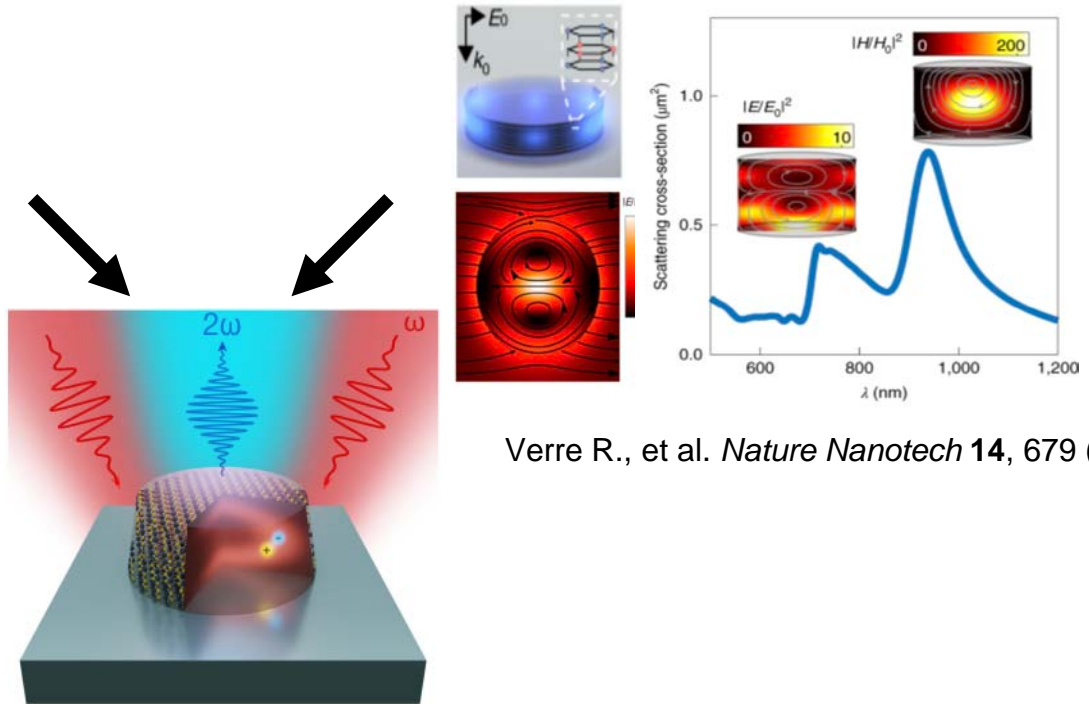
Mie-resonant dielectric photonics with 2D semiconductors

The nonlinear response of MoS₂ is enhanced near exciton wavelength



Trolle M.L. et al. *PRB* **92**, 161409 (2015)

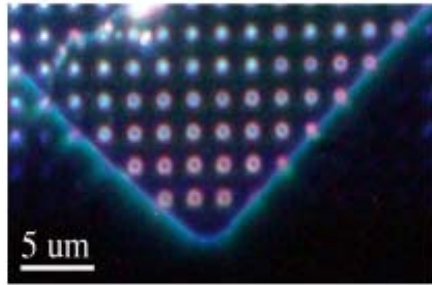
High refractive index of MoS₂ allow one to create the resonant structures



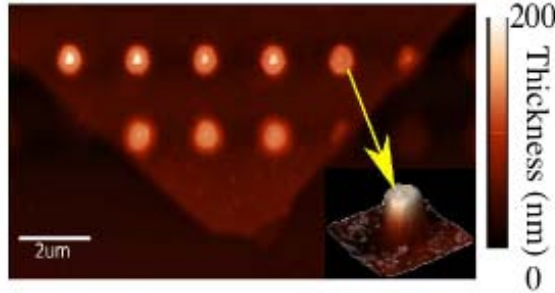
Verre R., et al. *Nature Nanotech* **14**, 679 (2019)

SHG enhancement by MD Mie-resonances at fundamental wavelength and exciton excitation on SHG wavelength

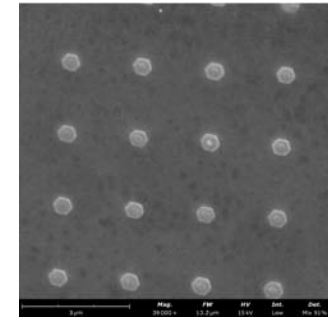
Mie-resonant dielectric photonics with MoS₂ nanodisks



Dark-field image

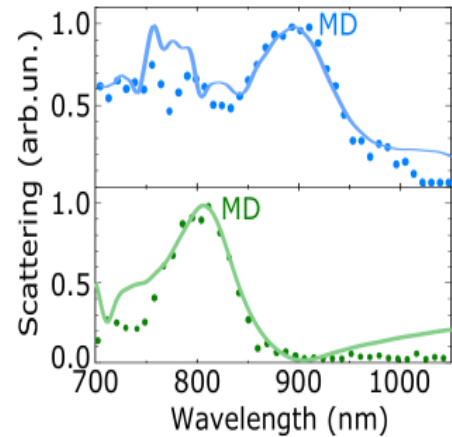
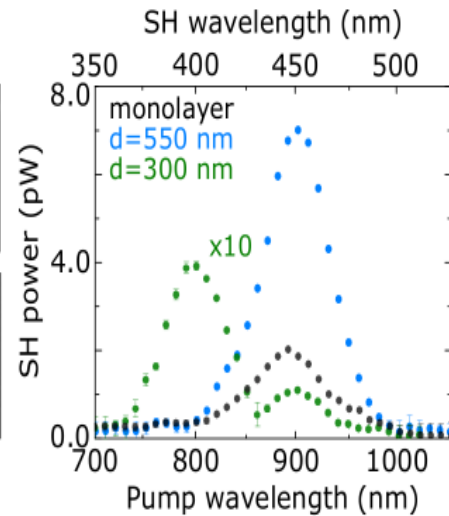
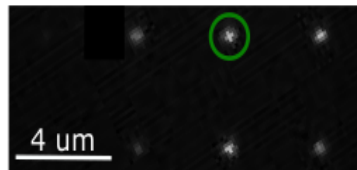
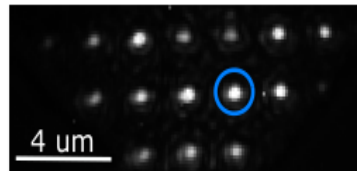


AFM



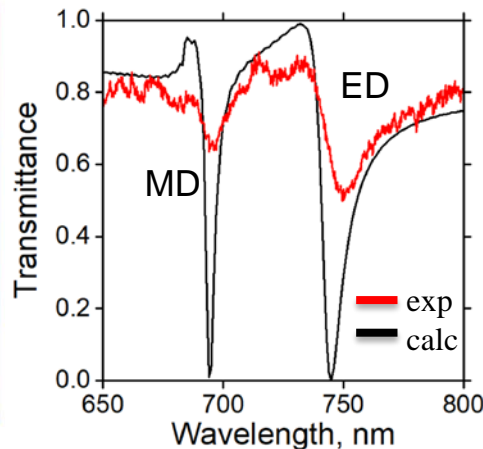
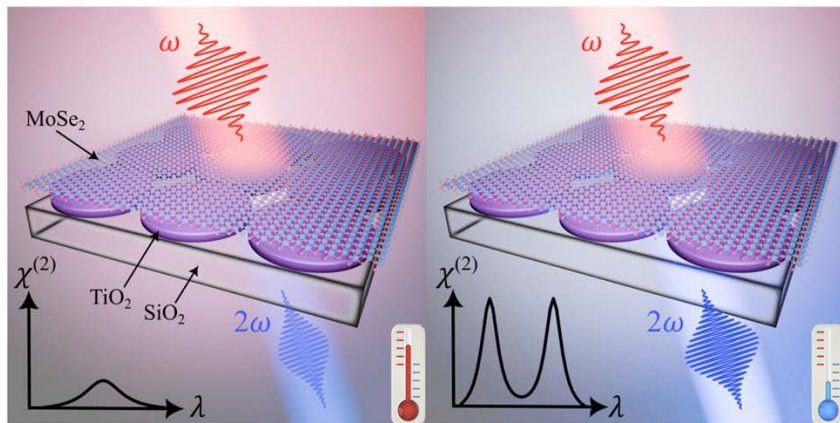
SEM

- 110 nm-thick exfoliated flake
- electron beam lithography
- reactive ion etching

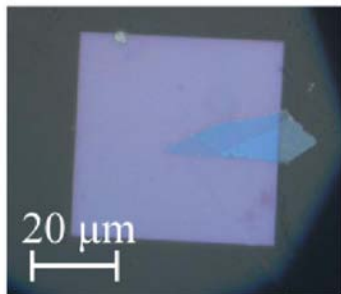
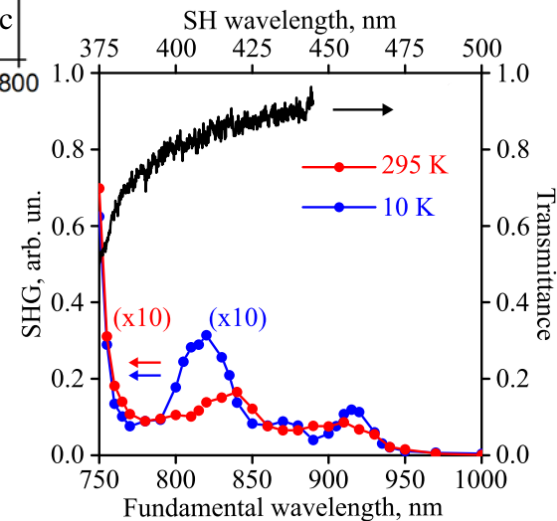


In the spectral region of the MD resonance, an increase in the SHG is observed

Cryogenic SHG enhancement of TMDC monolayer coupled with high-Q dielectric metasurface



Spectral overlapping of high-Q resonance with exciton



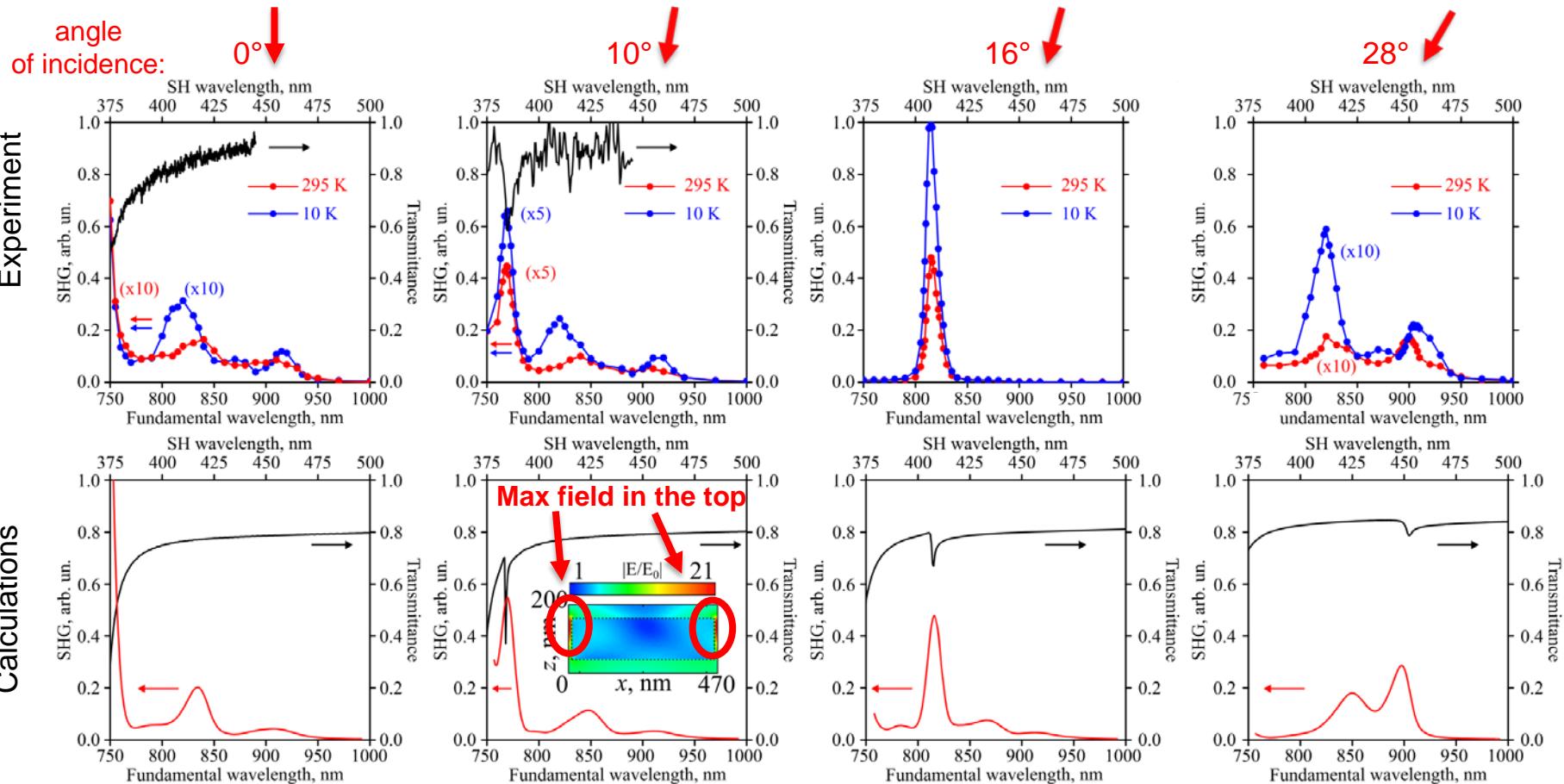
TiO₂

- dielectric
- low losses
- high refractive index (2.4)

MoSe₂

- exciton \sim 800 nm (1.5 eV)
- high $\chi^{(2)}$ values

Nonlinear spectroscopy of high-Q dielectric metasurface

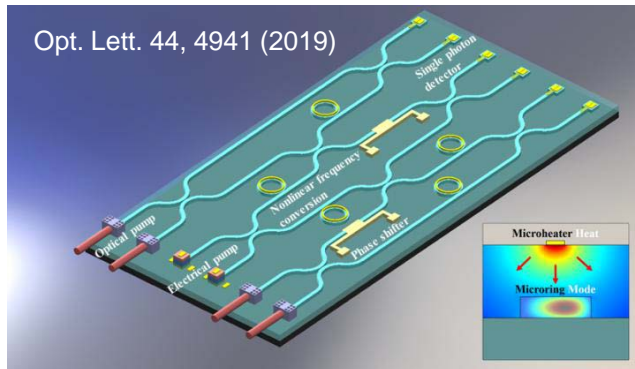


Фотоника и аналоговые вычисления

Преимущества фотоники

- Высокая тактовая частота
- Энергоэффективность
- Широкая полоса пропускания
- Помехоустойчивость

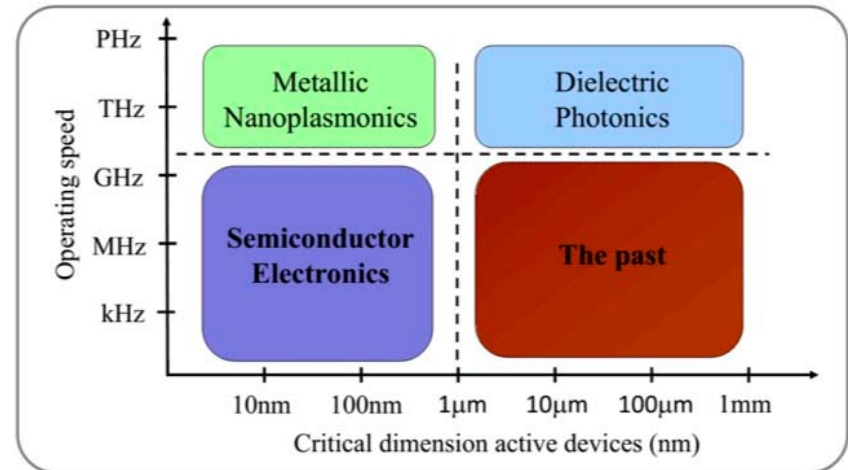
Интегральный фотонный чип



- Возможность миниатюризации элементов
- Усиление нелинейных эффектов за счет резонансов
- Структурные эффекты

Недостатки

- Размер элементов ограничен длиной волны
- Проблемы оптического хранения информации



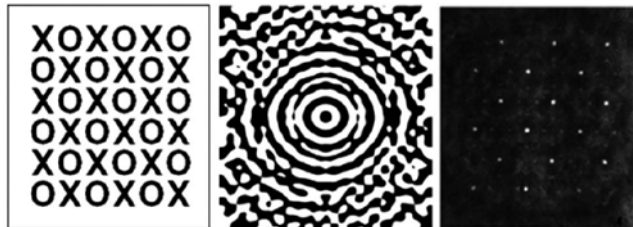
Метаповерхности для задач аналоговых вычислений

Устройства на основе метаповерхностей

- ахроматические металинзы
- генераторы голограмм
- фазовые корректоры
- пространственные модуляторы света

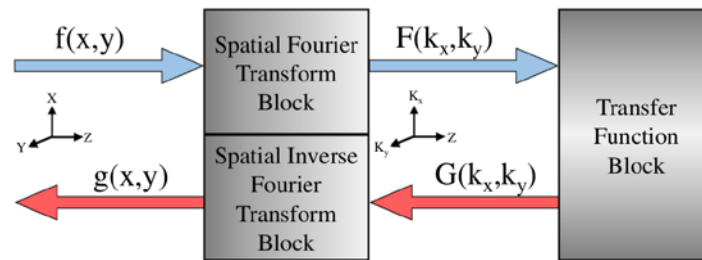


входное изображение Фурье-фильтр буквы "О" результат корреляции



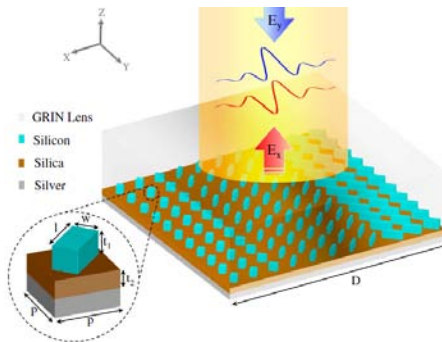
Применение метаповерхностей

- элементы сверточных нейронных сетей
- предобработка изображений
- выделение границ
- поиск опорных объектов на изображениях

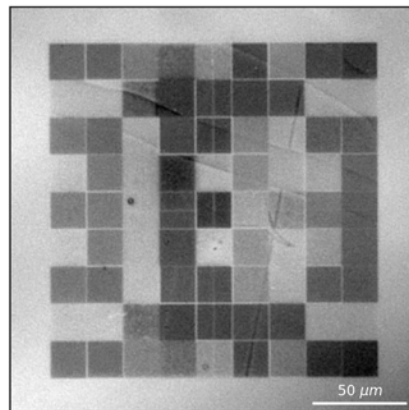
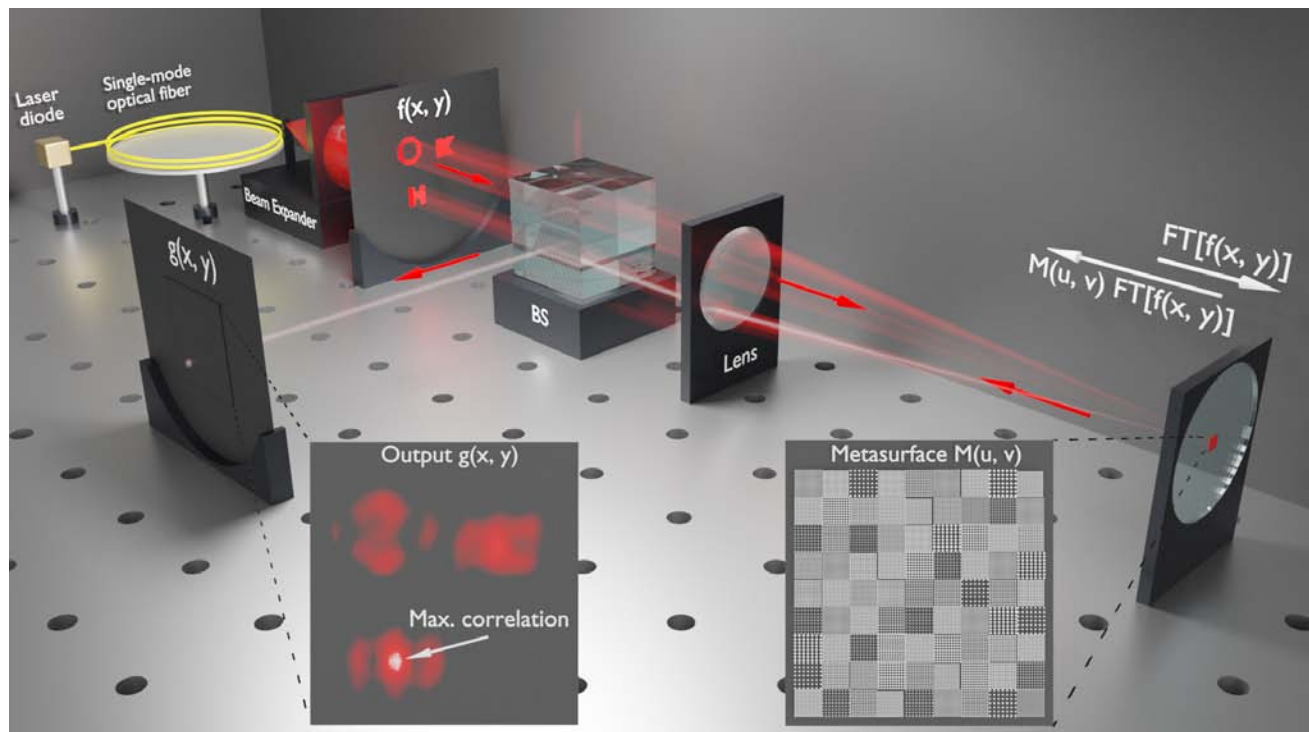


$$g(x, y) = h(x, y) * f(x, y) = \iint h(x - x', y - y') f(x', y') dx' dy'$$

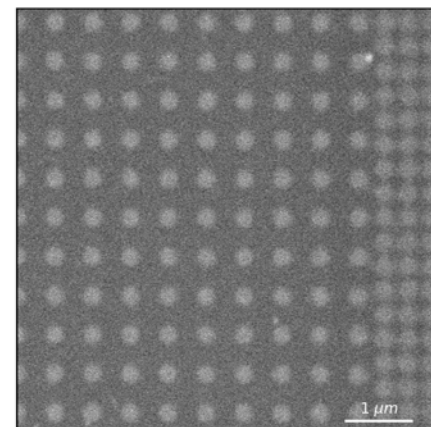
$$G(k_x, k_y) = H(k_x, k_y) F(k_x, k_y)$$



Fourier filtering system with a silicon metasurface

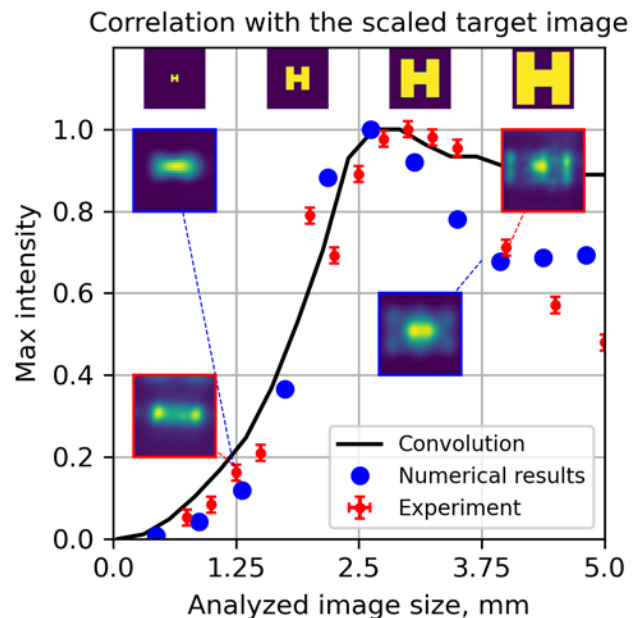


Bright-field microscope image of the whole metasurface



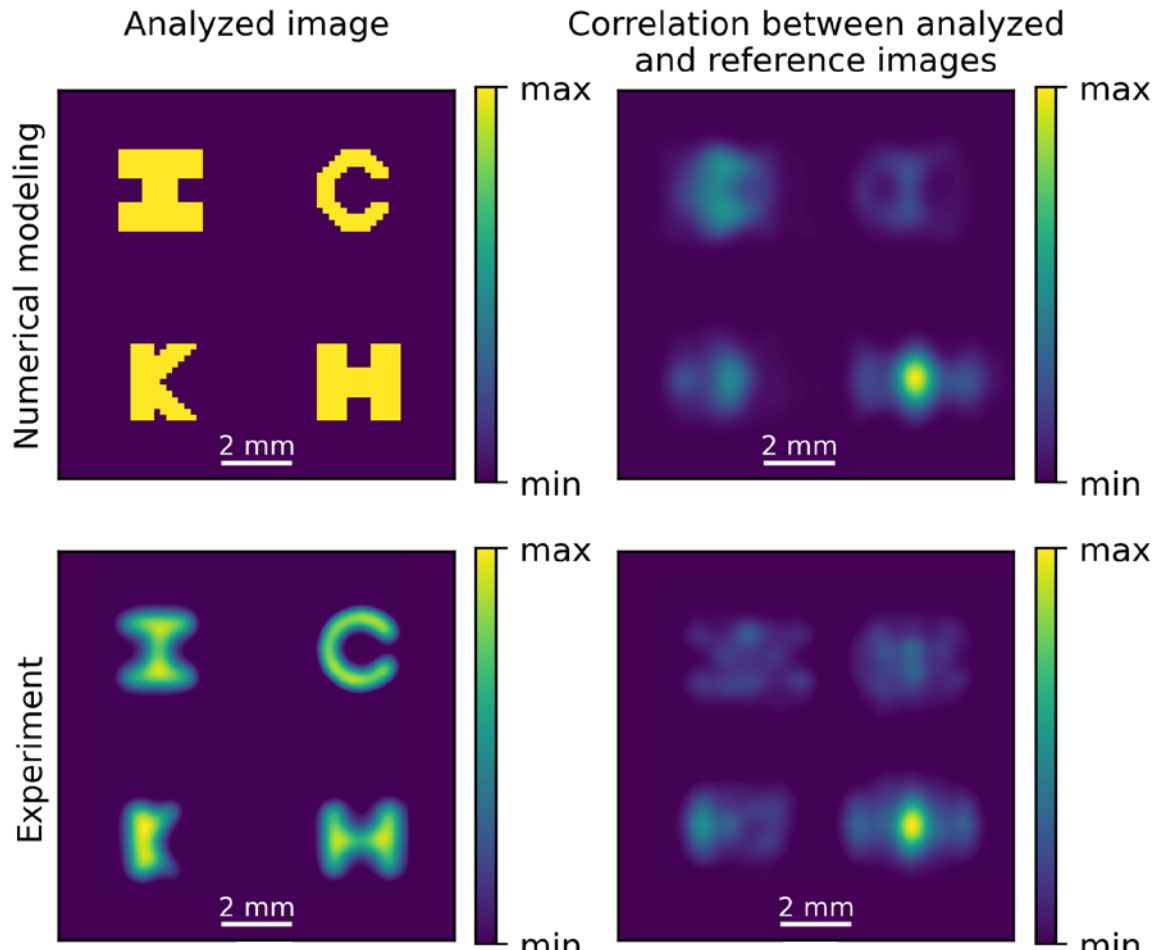
A SEM image of a region of the metasurface

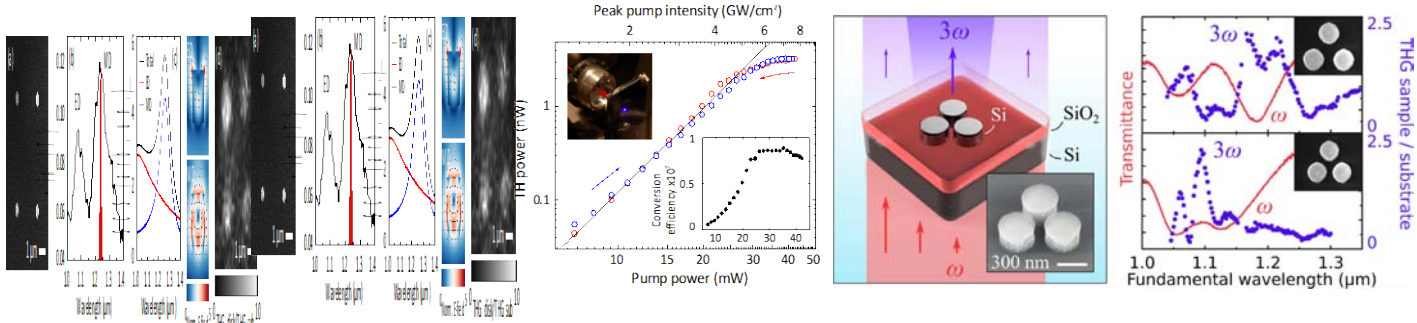
Fourier filtering system with a silicon metasurface



(top) Filtering of target images with different size.

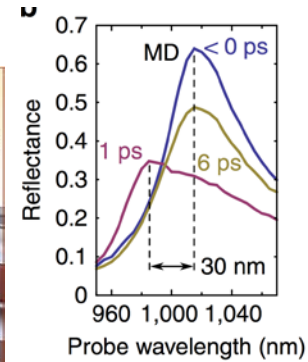
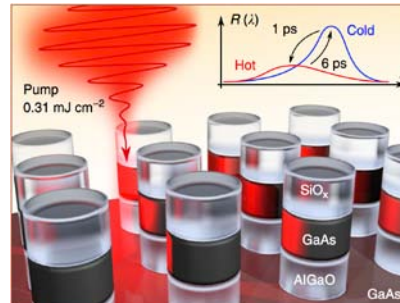
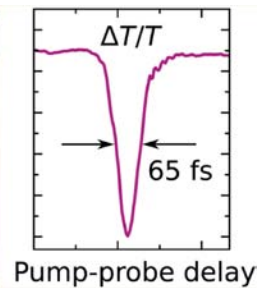
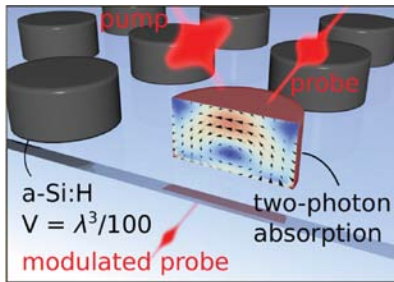
(right) Filtering an image containing different letters in the presence of the target image.





- [1] “Multifold Enhancement of Third-Harmonic Generation in Dielectric Nanoparticles Driven by Magnetic Fano Resonances,” *Nano Letters* **16**, 4857 (2016)
- [2] “Ultrafast all-optical tuning of direct-gap semiconductor metasurfaces,” *Nature Communications* **8**, 17 (2017)
- [3] “Enhanced nonlinear light generation in oligomers of silicon nanoparticles under vector beam illumination”, *Nano Letters* **20**, 3471 (2020)
- [4] “Analog optical correlation augmented by Mie-resonant metasurfaces”, *ACS Photonics* **11**, 2506 (2024)
- [5] “Cryogenic nonlinear microscopy of high-Q metasurfaces coupled with transition metal dichalcogenide monolayers ”, *Nanophotonics* **13**, 3429 (2024).

fedyanin@nanolab.phys.msu.ru



Acknowledgments

Boris Lukyanchuk, Alexander Shorokhov, Alexander Musorin, Varvara Zubyyuk, Vladimir Bessonov and many others



